Protein–lipid interactions in reconstituted high density lipoproteins: Apolipoprotein and cholesterol influence

ARTICLE *in* CHEMISTRY AND PHYSICS OF LIPIDS · NOVEMBER 2001

Impact Factor: 2.42 · DOI: 10.1016/S0009-3084(01)00176-1

4 AUTHORS, INCLUDING:

Alexander D Dergunov
National Research Center for Prevent…
72 PUBLICATIONS **384** CITATIONS
SEE PROFILE

Gérard Siest
University of Lorraine
654 PUBLICATIONS **14,240** CITATIONS
SEE PROFILE

ELSEVIER

Chemistry and Physics of Lipids
113 (2001) 67–82

CPL
CHEMISTRY AND PHYSICS OF LIPIDS

www.elsevier.com/locate/chemphyslip

Protein–lipid interactions in reconstituted high density lipoproteins: apolipoprotein and cholesterol influence

Alexander D. Dergunov [a,*], Gennady E. Dobretsov [b], Sophie Visvikis [c], Gerard Siest [c]

[a] *National Research Centre for Preventive Medicine, 10, Petroverigsky Street, 101953 Moscow, Russia*
[b] *Research Institute for Physical Chemical Medicine, 119828 Moscow, Russia*
[c] *Centre du Médicament et Centre de Médecine Préventive, Université Henri Poincaré et INSERM Unité 525, 30 rue Lionnois, 54000 Nancy, France*

Received 20 March 2001; received in revised form 2 July 2001; accepted 11 July 2001

Abstract

Two fluorescent probes—*cis*- and *trans*-parinaric acids were used to study the dimensions, lipid dynamics and apolipoprotein location in the reconstituted discoidal high density lipoproteins (rHDL). The rHDL particles made from apolipoprotein A-I (apoA-I), dipalmitoylphosphatidylcholine (DPPC), with or without cholesterol (Chol) were compared with the analogous particles with two other apolipoproteins-apoE and apoA-II. The data obtained for apoA-I-containing rHDL were as follows: (1) the inclusion of 8 mol.% of cholesterol did not significantly change the particle dimensions (13 ± 1 nm) or the mean distance between apoA-I and the disc axis; (2) the phospholipid domains—boundary lipid region in the close vicinity to apoA-I molecule and the remaining part of the bilayer—existed at temperatures both lower and above DPPC transition temperature T_t; (3) at $T < T_t$ Chol molecules preferentially accumulated in the central area with a radius of 2.8 nm that conserved partially after DPPC phase transition; (4) inhomogeneous cholesterol distribution was assumed to exist within these domains. A hydrophobic matching concept was used to compare protein–lipid interactions in rHDL particles. For complexes with all three apolipoproteins studied, at $T < T_t$ the probe mobility in the lipid phase of rHDL was significantly higher compared to pure DPPC bilayer. After temperature-induced transition, mobility increased significantly still being lower in rHDL. The comparative study of lipid dynamics in apoA-I-, apoE- and apoA-II-containing complexes revealed the presence of boundary lipid in all three complexes without cholesterol. The degree of cholesterol exclusion from the boundary lipid region seems to increase in the order A-I < E < A-II for Chol-containing complexes, the exclusion being an inherent property of the particular apolipoprotein molecule.

Abbreviations: apoA-I, apolipoprotein A-I; apoA-II, apolipoprotein A-II; apoE, apolipoprotein E; Chol, cholesterol; *cis*-PA, *cis*-parinaric acid; DPPC, dipalmitoylphosphatidylcholine; HDL, high density lipoproteins; NRET, non-radiative energy transfer; PC, phosphatidylcholine; PL, phospholipid; rHDL, reconstituted high density lipoproteins; *trans*-PA, *trans*-parinaric acid; T_t, phospholipid transition temperature.

* Corresponding author. Tel.: +7-95-927-0324; fax: +7-95-928-5063.
E-mail address: dergunov@img.ras.ru (A.D. Dergunov).

0009-3084/01/$ - see front matter
PII: S0009-3084(01)00176-1

Keywords: Apolipoprotein A-I; Apolipoprotein A-II; Apolipoprotein E; Non-radiative energy transfer; Protein–lipid interactions; Reconstituted HDL

1. Introduction

High density lipoproteins (HDL) are a complex system of various particles with different composition and origin which play a key role in reverse cholesterol (Chol) transport (Johnson et al., 1991; Fielding and Fielding, 1995), a major pathway in active cholesterol removal from peripheral cells. A minor fraction of total HDL population, the discoidal nascent particles, represents the most metabolically active pool. To overcome the structural and metabolic heterogeneity observed with native plasma HDL, reconstituted particles (Sparks et al., 1992a,b, 1993, 1995; Rye et al., 1998) composed of a particular apolipoprotein and phospholipid (PL), often with cholesterol added, are widely used in various physico-chemical (Jonas, 1992) and physiological (Meng et al., 1995) studies. Both compositional and dynamic aspects of PL–Chol interactions in rHDL, despite extensive study, still remain incompletely solved and four variable alternatives are postulated concerning the existence, stability and stoichiometry of the complex between Chol and PL molecules. These alternatives are: (1) a tight phosphatidylcholine (PC)–Chol complex as suggested by Presti et al. (1982a)and Presti et al. (1982b) although this static point of view was criticized (Yeagle, 1981); (2) a superlattice model (Virtanen et al., 1995; Wang et al., 1998), in which the superlattices are thought of as structures in which there are repulsions between cholesterol molecules which are positioned remotely on presumed lattice sites; (3) a molecular interaction concept (Ipsen et al., 1987), in which the phase behavior of PC–Chol mixtures was based on the assumptons: cholesterol interacts favourably with phosphatidylcholine chain in an extended conformation and cholesterol disturbs the translational order in the gel state of phosphatidylcholine; (4) a most sophisticated model of the 'condensed complex' which included *two* immiscibility regions in the phase diagram of Chol–PL mixtures (Radhakrishnan and McConnell, 1999; Radhakrishnan et al., 2000) developed for the binary and ternary mixtures of cholesterol and some phospholipids with long saturated acyl chains such as sphingomyelin.

The presence of more than 7–10 mol.% cholesterol resulted in phase separation with the formation of separate Chol-rich or *lo*-phase (Ipsen et al., 1987) and Chol-poor phases evidenced by calorimetry (McMullen et al., 1993; McMullen and McElhaney, 1995; Vist and Davis, 1990) and ^{2}H NMR spectroscopy (Vist and Davis, 1990). (In the 'condensed complex' model the simultaneous presence of three coexisting liquid phases allows an additional condensed complex phase.) Above 20–25 mol.% Chol content in dipalmitoylphosphatidylcholine (DPPC) bilayer only Chol-rich phase seemed to exist (McMullen et al., 1993; Sankaram and Thompson, 1990; Vist and Davis, 1990). In the case of Chol-containing DPPC bilayers, the immiscibility was observed both for gel (McMullen et al., 1993; McMullen and McElhaney, 1995; Vist and Davis, 1990) and fluid (Sankaram and Thompson, 1990; Vist and Davis, 1990) phases and *lo*-phase and DPPC-rich phase became miscible at a critical temperature above the main gel to fluid phase transition temperature (Ipsen et al., 1987; Sankaram and Thompson, 1990). However, the existence of separate Chol-rich phase did not accord with the uniform distribution of fluorescent Chol analogue in palmitoyloleoylphosphatidylcholine bilayer (Hyslop et al., 1990) and with homogeneous ESR spectra of PL-like spin probe in any binary mixture of cholesterol with dimyristoyl-, dipalmitoyl- and distearoylphosphatidylcholines (Sankaram and Thompson, 1990) that led authors to suggest a fast exchange between phases, i.e. that neither phase was long-lived.

Besides compositional features, the dynamic nature of PC–Chol interactions is of great importance. There is general agreement that cholesterol induces the condensing/ordering effect in a fluid

state of the 'condensable' phospholipid, i.e. saturated phosphatidylcholines and sphingomyelin. The Chol effect is much weaker for 'non-condensable' phospholipids, mainly polyunsaturated PC. The uncoupling observed in motional parameters for PC and Chol (Gliss et al., 1999; Yeagle, 1981) does not coincide with the long-lived complex model.

Various aspects of protein–lipid interactions such as the strength, lipid sorting and selectivity at protein surface, protein–lipid phase equilibria are described accurately by hydrophobic matching concept (Mouritsen and Bloom, 1984). This concept predicts that the free energy of a membrane will be reduced as the difference between the hydrophobic length of protein and phospholipid acyl chains is reduced. Lipid molecules are believed to adapt mostly through the lipid chain order and/or transition temperature changes (Dumas et al., 1999; Gil et al., 1998; Killian, 1998). Alternate models of the relative location of the lipid and apolipoprotein constituents in rHDL were suggested (Borhani et al., 1997; Brasseur et al., 1992; Segrest, 1977; Segrest et al., 1999).

To investigate the nature of lipid–lipid and protein–lipid interactions, we began recently a systematic study of the structure and molecular dynamics of rHDL particles composed from principal HDL apolipoprotein-apoA-I and DPPC with the aid of fluorescent probes. The probes, *cis*-parinaric (*cis*-PA) and *trans*-parinaric acid (*trans*-PA), sense the co-existing gel and liquid–crystalline lipid phases differently (Dergunov et al., 1997; Dobretsov et al., 1998; Dergunov and Dobretsov, 2000). In the present investigation, we studied the effect of cholesterol and three major HDL apolipoproteins, apoA-I, apoE and apoA-II, on the dimensions and the lipid dynamics in rHDL discoidal particle formed with a single apolipoprotein. The dimensions of apoA-I-containing complexes and exact apolipoprotein location on the disc periphery were measured. The preferential cholesterol distribution into the central part of the discoidal apoA-I/DPPC/Chol complex was suggested. The different Chol distribution between two lipid regions, i.e. central area and boundary lipid, seems to exist in rHDL with different apolipoproteins and not to depend on the complex dimensions but rather on the apolipoprotein structure. As far as we know, this is the first attempt to apply the hydrophobic matching concept to compare protein–lipid interactions in rHDL with different apolipoproteins both in the presence and in the absence of cholesterol.

2. Materials and methods

2.1. Materials

Dipalmitoylphosphatidylcholine and cholesterol were purchased from Sigma (MO, USA). ^{3}H-labelled cholic acid was purchased from NEN (MA, USA). Fluorescent probes *cis*- and *trans*-parinaric acids were purchased from Molecular Probes (OR, USA) and stored in the freezer in an ethanol solution (about 0.5 mM) until use. Apolipoproteins A-I and A-II were isolated from delipidated human plasma high density lipoproteins (Van Tornout et al., 1980). Apolipoprotein E was purified from pooled human plasma very low density lipoproteins (Dergunov et al., 1990). The purity of apolipoproteins was checked by SDS-PAGE (Laemmli, 1970) in a 8–25% precast gel (Pharmacia LKB Phast System) or in a 5–20% gel prepared in the laboratory. Generally, the purity was greater than 95%. The buffer used throughout this study was 50 mM Tris–HCl, pH 8.0, 0.15 M NaCl, 0.02% NaN_3.

2.2. Methods

2.2.1. Preparation and characterization of apolipoprotein/DPPC recombinants with different apolipoproteins and apoA-I/DPPC/Chol complexes with different apoA-I content

Discoidal rHDL were prepared by a procedure described previously (Dergunov et al., 1997). Protein and lipid recoveries were generally greater than 70%. The efficiency of cholate removal was greater than 99.5% as estimated from a control experiment by inclusion of a tracer quantity of ^{3}H-cholic acid into the initial mixture, i.e. complexes after Bio-Beads procedure contained less than 2 mol.% cholate relative to DPPC content.

This cholate content did not differ significantly from the values for apoA-I-containing complexes prepared analogously (Sparks et al., 1992b) or by dialysis procedure Matz and Jonas, 1982) and interfered in a negligible manner with phase (Van Erpecum and Carey, 1997) or dynamic (Schubert et al., 1986) properties of PL–Chol mixtures. After cholate removal, complexes were reisolated by gel-filtration on a Superose 6PG (1.0 × 48.5 cm) column. The chemical composition and dimensions of the isolated complexes were determined as described (Dergunov et al., 1997).

The same procedure was used to prepare four apoA-I/DPPC/Chol complexes with different apolipoprotein content but trying to keep DPPC/Chol ratio constant. The initial DPPC/apoA-I molar ratios were 402:1, 253:1, 150:1 and 100:1. In this case, the apoA-I content was estimated by determination of phenylalanine by HPLC after protein hydrolysis (Brasseur et al., 1990). To increase the separation, complexes were isolated on two identical Superose 6PG columns connected in series. For larger complexes, the elution profiles became more heterogeneous and, to isolate mainly one population of the particles, the profiles were deconvoluted by eye into 3–4 components. The tube material with absorbance/fluorescence values not smaller than one-half of the corresponding peak, was combined for subsequent procedures.

2.2.2. Liposome preparation

The procedure was described in our previous paper (Dergunov et al., 1997).

2.2.3. NRET study: model of rHDL and experimental measurements

A discoidal shape of the complexes of apoA-I with DPPC both in the absence and in the presence of cholesterol is assumed to exist. For our purpose, the particle consists of three parts, i.e. lipid, donor and acceptor zones which can overlap partially. The lipid molecules fill the cylinder with the radius R. The tryptophan residues of apoA-I serve as donor groups and lipid-embedded *trans*- or *cis*-PA as acceptors. The donor groups occupy the volume between the surfaces of two cylinders with the internal and external radii RD_{int} and RD_{ext}, respectively (Fig. 1). Parameters of the acceptor localization RA_{int} and RA_{ext}, different for each probe, are indicated on the same figure. Below, $RA1_{int}$ and $RA1_{ext}$ values belong to *trans*-PA and $RA2_{int}$ and $RA2_{ext}$ to *cis*-PA, respectively. These values were assumed to vary and they were obtained as a result of the optimization procedure. It should be stressed that this model is valid only for discoidal, not for spherical rHDL particles, quite different formalism has to be applied in the latter case.

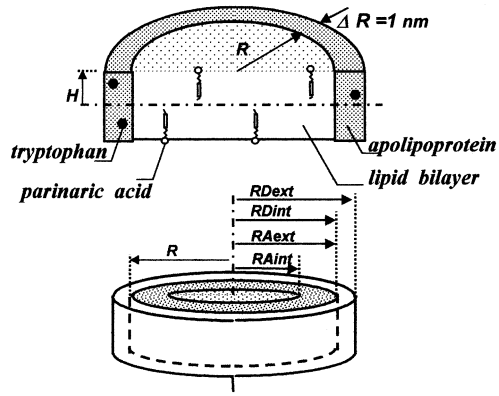

Fig. 1. Model of rHDL structure. The inner lipid phase in the form of cylinder is surrounded by a protein shell. The apolipoprotein A-I trypthophan residues serve as energy donors in NRET study. The donor location is described by four parameters, i.e. height H, internal and external radii RD_{int} and RD_{ext}, respectively and the thickness of the donor shell ΔRD. The lipid-embedded parinaric acid probes serve as energy acceptors and their location is described by two parameters, i.e. internal and external radii RA_{int} and RA_{ext}, respectively. The parinaric chromophore group indicated as a small box lies between 0.5 and 1.2 nm from the plane between two lipid layers.

Table 1
Förster's radius R_o for energy transfer from apolipoprotein A-I to parinaric acids in rHDL

Sample	Probe	R_o, (nm)	
		25 °C	50 °C
A-I/DPPC	*cis*-PA	3.60	3.46
	trans-PA	3.41	3.42
A-I/DPPC/Chol	*cis*-PA	3.69	3.46
	trans-PA	3.49	3.42

The values of Förster' radius R_o were calculated as earlier (Dobretsov et al., 1998) (Table 1) and no strong dependence of R_o on temperature was observed. The R_o values were calculated with tryptophan fluorescence decay time averaged as 4.4 ns at 20 °C (Davidson et al., 1996, 1999; Mantulin et al., 1986). We assume a random mutual orientation of donor and acceptor groups as: (i) there are eight donor tryptophan residues in each rHDL particle and there seems no reason to suggest any prefential chromophore orientation; (ii) trypthophan fluorescence is largely depolarized due to the existence of two orthogonal electronic transitions in this chromophore; (iii) donor groups possess fast thermal motion with the rotation correlation time 0.2–0.4 ns (Davidson et al., 1999) small enough compared to the decay time as 4–5 ns; and (iv) acceptor groups rotate also with high frequency at temperatures both lower and above phospholipid transition temperature within an angle larger than 30°.

The measurements were done on an Aminco SPF-500 spectrofluorometer equipped with a polarizer accessory. ApoA-I-containing complexes (200 μM as DPPC) in a total volume 400 μl were titrated at 25 and at 50 °C with increasing quantities of *cis*- and *trans*-PA added from concentrated ethanol solution. The final ethanol concentration at the end of the titration did not exceed 1%. Fluorescence of Trp residues was excited at 280 nm and area F under the emission curve at the range of 300–350 nm was considered to be proportional to the fluorescence quantum yield. The efficiency of the energy transfer between apoA-I tryptophanyls and parinaric acid probe molecules is calculated from the quenching of the donor emission. At the sequential probe addition to rHDL solution the F value decreased and a set of $n+1$ experimental values Fe[0], …, Fe[i], …, Fe[n] was obtained which corresponded to the acceptor concentrations in a lipid-bound form Ca[0], …, Ca[i], …, Ca[n] (mol/l, Ca[0] = 0). The corresponding experimental errors were as Er[0], …, Er[i], …, Er[n]:

$$\mathrm{Er}[i] = \left[\frac{1}{k\,(k-1)}\sum_{j=1}^{j=k}(\mathrm{Fe}_j[i] - \mathrm{Fe}[i])^2\right]^{1/2}, \qquad (1)$$

where Fe[i] is the mean value for a set of $\mathrm{Fe}_j[i]$ values from k separate experiments ($j = 1, \ldots, k$) at the particular acceptor concentration Ca[i].

The set of calculated values of Fm[0], …, Fm[i], …, Fm[n] for the corresponding acceptor concentrations was obtained using the procedure (Dobretsov et al., 1998) to fit NRET data to the dimensions of rHDL within the model described above. To evaluate the accuracy of the fitting procedure, a least-squared criterion was used:

$$\chi^2 = \frac{1}{n}\sum_{i=1}^{i=n}\left[\frac{(\mathrm{Fm}[i] - \mathrm{Fe}[i])}{\mathrm{Er}[i]}\right]^2. \qquad (2)$$

For the optimization routine to be valid, χ^2 values have not to be more than 1 and any improvement of the model results in the decrease of χ^2 parameter.

2.2.4. Temperature-induced phase transition

The thermal mobility of lipid molecules nearest to the probe molecules influences both fluorescence intensity and anisotropy. To monitor temperature-induced phase transitions in the liposome and in the complexes, the sample in the cuvette (200 and 750 μM DPPC for complex and for liposome, respectively) with 4 μM *cis*- or *trans*-PA was placed into the cell chamber preheated to 55 °C, and the temperature was gradually decreased to 25 °C at a rate 0.7°/min while measuring fluorescence intensity at fixed time intervals. For both probes, excitation was at 320 nm with 0.5 nm excitation slit, and emission was recorded at 420 nm with 10 nm slit. Total intensity F and anisotropy r values were calculated as:

$$F = F_{\parallel} + 2F_{\perp}, \qquad (3)$$

$$r = \frac{F_{\parallel} - F_{\perp}}{F_{\parallel} + 2F_{\perp}}. \qquad (4)$$

$F_{\parallel}$ and $F_{\perp}$ refer to parallel and perpendicular orientation of polarizer in an emission beam relative to the polarizer in an excitation beam, respectively. No correction for instrumental polarization was made as G-factor (Lakowicz, 1983) of the instrument was nearly 1. Anisotropy values were used to estimate the amplitude of wobbling-type motion of the probe molecule inside the conical

volume described by the 2γ angle in the lipid phase (Kinosita et al., 1977):

$$r_\infty/r_0 = (0.5\cos\gamma \times (1+\cos\gamma))^2, \quad (5)$$

where r_∞ and r_0 are the infinite and zero time anisotropy values and measured r value was used instead of r_∞ to obtain the lowest estimate of γ angle. For parinaric acid probes, the r_0 value can be choosen as 0.35 (Sklar et al., 1979).

The data were treated by nonlinear least squares using the SAS package as a first order phase transition to obtain transition temperature T_t and the ratio of the probe fluorescence intensities F_s/F_f and anisotropies r_s/r_f at the beginning and after the completion of the phase *trans*ition ('s'-solid, 'f'-fluid):

$$F = \frac{F_{0s} + aT + (F_{0f} + bT)\, e^{(-\Delta H^0_{sf} + T\Delta S^0_{sf})/RT}}{1 + e^{(-\Delta H^0_{sf} + T\Delta S^0_{sf})/RT}}, \quad (6)$$

$$r = \frac{(r_{0s} + cT)(F_{0s} + aT) + (r_{0f} + dT)(F_{0f} + bT)\, e^{(-\Delta H^0_{sf} + T\Delta S^0_{sf})/RT}}{F_{0s} + aT + (F_{0f} + bT)\, e^{(-\Delta H^0_{sf} + T\Delta S^0_{sf})/RT}}, \quad (7)$$

where F_{0s} (r_{0s}) and F_{0f} (r_{0f}) is the fluorescence intensities (anisotropies) of the probe in solid and fluid lipid at some reference temperature; $a(c)$ and $b(d)$ is the temperature dependence of the fluorescence (anisotropy) of the probe in solid and fluid lipid (i.e. baseline slope, assumed to be linear); ΔH^o_{sf} and ΔS^o_{sf} is the enthalpy and entropy changes for the (two-state) phase transition. The transition temperature, T_t, equals $\Delta H^o_{sf}/\Delta S^o_{sf}$.

3. Results

3.1. The dimensions of apoA-I/DPPC/Chol complexes and localization of trans- and cis-PA

It followed from our previous study (Dergunov and Dobretsov, 2000) that discoidal rHDL particle had a radius of the lipid phase R as 5.0–5.2 nm and an apolipoprotein shell of 1 nm at the disc periphery. We postulated that the addition of 8 mol.% cholesterol did not perturb significantly the apolipoprotein structure and the thickness of apolipoprotein shell $\Delta RD = (RD_{ext} - RD_{int})$ was fixed as 1 nm. The thickness of the lipid bilayer

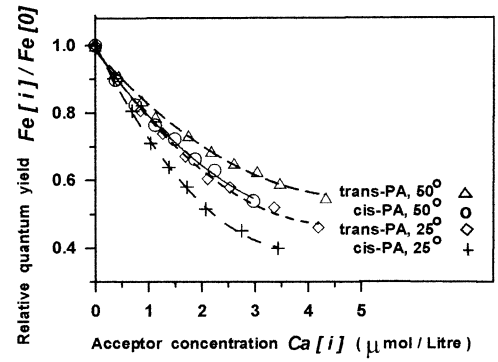

Fig. 2. The concentration dependence of the energy transfer between trypthophan residue(s) and parinaric acid probes in cholesterol-containing rHDL at 25 and 50 °C.

$2H$ was 4 nm, a value for DPPC bilayer (Keough and Davis, 1979) but 10% variations did not change significantly energy transfer. The transverse location of parinaric acid chromophores was the same as previously (Dobretsov et al., 1998; Dergunov and Dobretsov, 2000). However, the lateral location of the probe molecules in plane of the bilayer, the particle radius and/or the distance between particle axis and the apolipoprotein molecule were assumed to be sensitive to DPPC phase state and to cholesterol addition; the corresponding parameters were allowed to vary within our model.

In energy transfer study, apolipoprotein tryptophan residues and parinaric probe molecules serve as energy donors and acceptors, respectively. Upon probe addition, apoA-I fluorescence intensity decreased (Fig. 2). Comparison of these quenching curves with the analogous data for apoA-I/DPPC complexes without cholesterol (Dobretsov et al., 1998; Dergunov and Dobretsov, 2000) revealed a striking difference, i.e. the relative geometry of donor–acceptor pair changed. The radius of the lipid phase of rHDL particle cannot be smaller than 5.4 nm as followed from the treatment of *cis*-PA data obtained at $T < T_t$ (Fig. 3). It should be mentioned that the radius of the particles without cholesterol was close to 5.0–5.2 nm (Dobretsov et al., 1998; Dergunov and Dobretsov, 2000) and Chol addition did not significantly change the hydrodynamic dimensions of

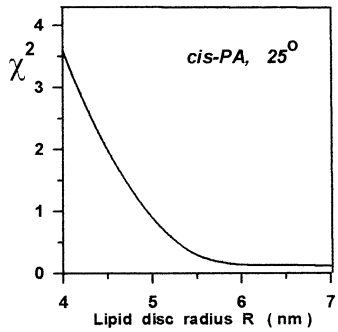

Fig. 3. Optimization of the lipid disc radius R in cholesterol-containing rHDL at 25 °C on the basis of the energy transfer from apoA-I to *cis*-PA. The χ^2 values were calculated for the optimal combination of the $RA2_{int}$ and $RA2_{ext}$ acceptor parameters at a given R value. The best parameter set is fixed as $RA2_{int} = 4.4$ nm and $RA2_{ext} = 5.4$ nm at $R = 5.4$ nm.

the particles (Dergunov et al., 1997). Small (0.25 nm) Chol-induced increase of particle radius has been observed by Sparks et al. (1992a) using electron microscopy. So, an R value of 5.4 nm for Chol-containing particles at $T < T_t$ was choosen.

Parametric fitting of *cis*-PA localization in rHDL ($RA2_{int}$ and $RA2_{ext}$) at $T < T_t$ (Fig. 4) to the experimental data corresponded to the exclusion of probe molecules from the central part of the particle. The radius of this inaccessible area was 3.5–4 nm and did not change if the R value was allowed to vary. The same location of *cis*-PA molecules on the disc periphery was obtained for particles without cholesterol (Dobretsov et al., 1998). Treatment of the data for *trans*-PA at $T < T_t$ (Fig. 5a) revealed an analogous peripheral location of probe molecules in the region from 2 to 5.4 nm, opposite to the central location of *trans*-PA in the particles without cholesterol (Dobretsov et al., 1998). After phase transition, *trans*-PA occupies a large part of the lipid phase except the narrow region (5–5.4 nm) at the disc periphery (Fig. 5b), while *cis*-PA molecules exclude from the central area where $RA2_{int}$ is 1.5–2 nm (Fig. 4). It should be stressed that at $T > T_t$ in the particles without cholesterol both probes occupy the whole lipid phase of the particle (Dobretsov et al., 1998); so, cholesterol incorporation is believed to induce the formation of a specific central area in the lipid phase at $T < T_t$ with a radius of 2.8 nm (as a mean for *trans*-PA and *cis*-PA distribution) involving 30% of the total DPPC molecules. After phase transition, this inaccessible area partially decreased but some *cis*-PA-inaccesible region with a radius of 1.5–2 nm remained.

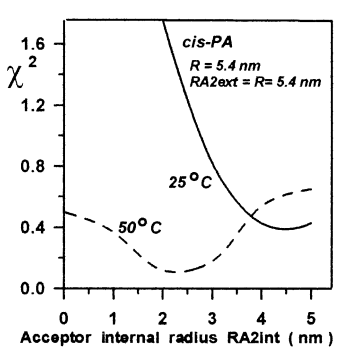

Fig. 4. The localization of ?*is*-PA in cholesterol-containing rHDL at 25 and 50 °C. The radius of the lipid phase R was fixed as 5.4 nm. The acceptor internal radius $RA2_{int}$ was varied at fixed $RA2_{ext}$ value as 5.4 nm.

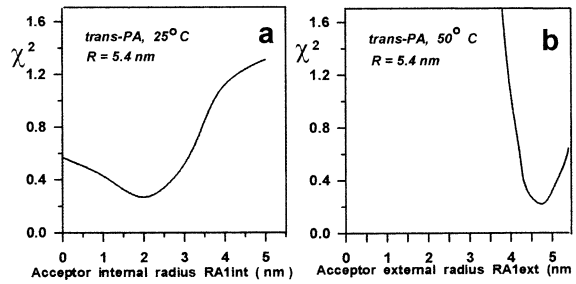

Fig. 5. The localization of *trans*-PA in cholesterol-containing rHDL. The radius of the lipid phase R was fixed as 5.4 nm. (a) the acceptor internal radius RA_{int} was varied while $RA1_{ext}$ was fixed at 5.4 nm at 25 °C; (b) the acceptor external radius $RA1_{ext}$ was varied while $RA1_{int}$ was fixed at 0 nm at 50 °C.

Moreover, it is possible that lateral distribution of cholesterol in the particle is not a random one. If *trans*-PA excludes from DPPC–Chol region at $T < T_t$, the cholesterol molecules should occupy the particle central area. At $T < T_t$, cholesterol addition resulted in decreased incorporation of both probes into the lipid phase as measured by the probe partition between water and lipid phases (Dergunov et al., 1997). The 30% decrease in the partition coefficient appeared to coincide with the dimensions of Chol-enriched region as

determined by NRET measurements. After DPPC phase transition, a larger part of the lipid phase became accessible for both probes and, as a result, a nearly 2- and 1.5-fold increase in partition coefficients was obtained for *trans*- and *cis*-PA incorporation into the Chol-containing complexes. However, the Chol-rich central region may still exist at temperatures higher than T_t.

3.2. Cholesterol influence on DPPC phase behaviour in liposomes

In DPPC liposomes without Chol, there was a sharp ($\Delta T = 2°$) temperature-induced phase transition with transition temperatures T_t calculated from fluorescence intensity and anisotropy of *trans*-PA as 41.48 and 40.82 °C, respectively; a less cooperative transition ($\Delta T = 5°$) shifted to the low temperature region by 0.4–0.6° was detected with *cis*-PA (Figs. 6 and 7, Table 2). These data agree well with the T_t values for DPPC obtained by differential scanning calorimetry (McMullen et al., 1993) and by fluorescence measurements with the same probes (Sklar et al., 1977, 1979). The values of fluorescence anisotropy for *cis*-PA were lower than for *trans*-PA over the whole temperature range studied which agrees with the data of Sklar et al. (1979) and suggests the existence of a solid domain(s) even at temperatures above T_t. Cholesterol inclusion in liposomes resulted in three major effects (Figs. 6 and 7, Table 2). Firstly, transition amplitude decreased with corresponding transition broadening as evidenced both by F and r measurements mostly with *trans*-PA.

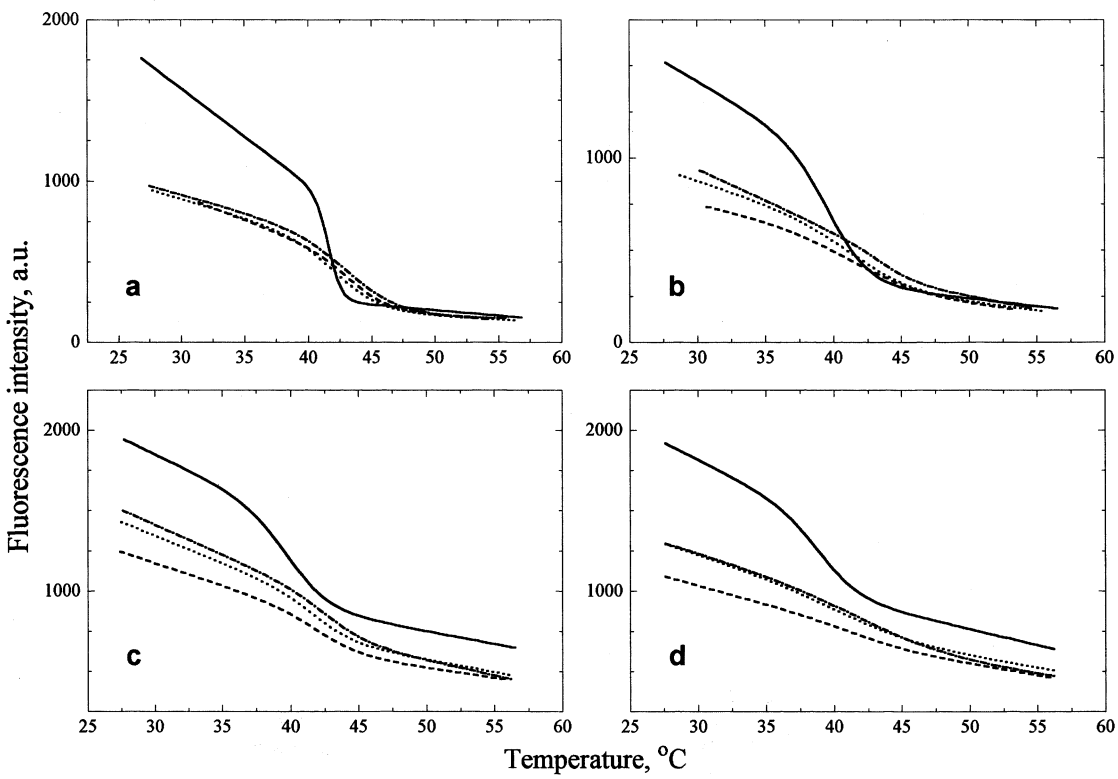

Fig. 6. Temperature responce of the fluorescence intensity of *trans*-PA (a, b) and *cis*-PA (c, d) in liposomes and in the complexes with different apo's in the absence (a, c) and in the presence of Chol (b, d) in preparations. The lines are the results of nonlinear curve fitting for the two-state phase transition model: (—), liposomes; (– – –), apoA-I-complexes; (- -), apoA-II-complexes; (···), apoE-complexes. Excitation was at 320 nm and emission recorded at 420 nm for both probes with polarizer accessory was calculated as $F = F_{\parallel} + 2F_{\perp}$, $F_{\parallel}$ and $F_{\perp}$ refer to parallel and perpendicular orientation of polarizer and analyzer, respectively.

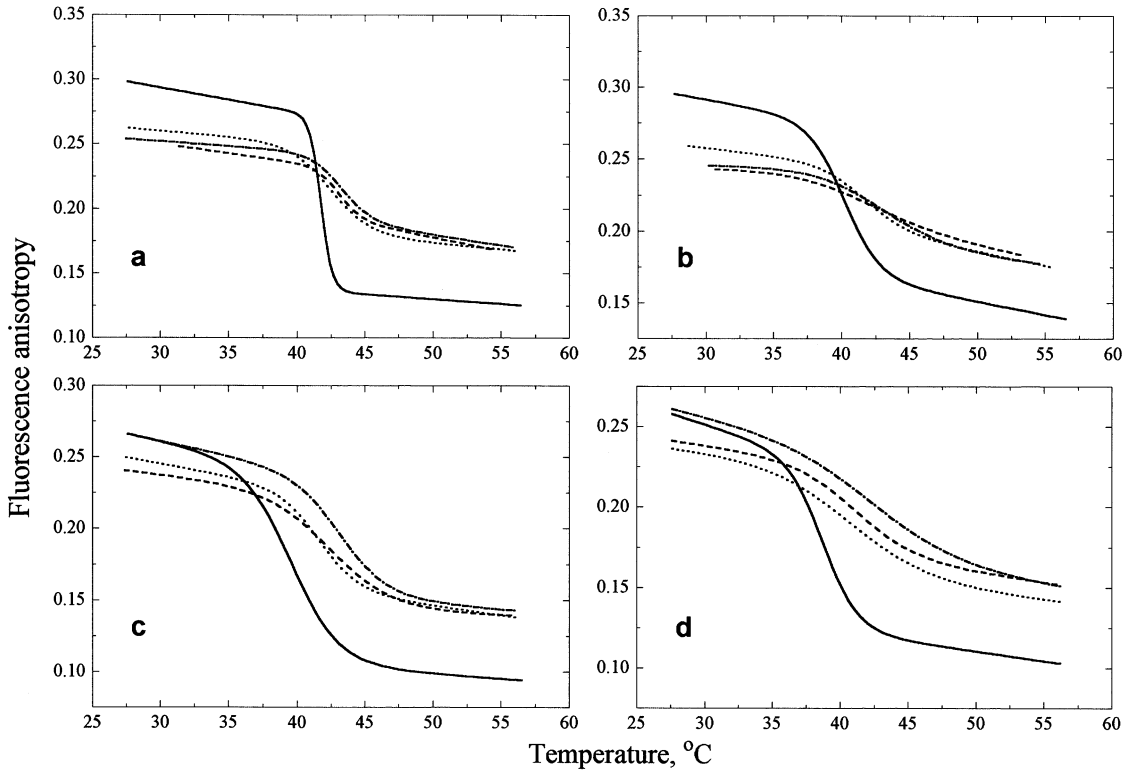

Fig. 7. Temperature responce of the fluorescence anisotropy of *trans*-PA (a, b) and *cis*-PA (c, d) in liposomes and in the complexes with different apo's in the absence (a, c) and in the presence of Chol (b, d) in preparations. Fluorescence anisotropy was calculated as $r = (F_{\parallel} - F_{\perp})/(F_{\parallel} + 2F_{\perp})$. For experimental details, see Fig. 6.

These effects related to the decrease of transition entropy may be indicative of Chol-induced disappearence of long-range order in the DPPC gel phase (Ipsen et al., 1987) preferably sensed by *trans*-probe. Secondly, the transition temperature decreased by 1.2° with *trans*-PA while only 0.3° with *cis*-PA. Again, this may correspond to the increased sensitivity of *trans*-PA compared to *cis*-PA to a presence of highly ordered DPPC state. If both Chol- and DPPC-rich phases are present in the gel state, then, from the direction of T_t change, the preferential location of *trans*-PA in the DPPC-rich phase with slighty lowered transition temperature (McMullen et al., 1993) may be suggested. Finally, Chol-induced decreased mobility of both parinaric acid probes at $T > T_t$ was observed and closely corresponded to the data obtained for DPPC bilayer (Rodriguez et al., 1997) and for other phospholipids (Ipsen et al., 1987; Vist and Davis, 1990).

3.3. Lipid phase state in rHDL with different apolipoproteins

Temperature-induced responses of fluorescent parameters in rHDL were treated to visualize apolipoprotein effect on: (i) the transition amplitude and cooperativity; (ii) phase transition temperature; and (iii) lipid dynamics in the presence and absence of cholesterol. The formation of a binary complex of specific apolipoprotein with DPPC suppressed the amplitude and cooperativity of the transition detected by fluorescence intensity of both probes (Fig. 6). This response was largely due to the decrease of quantum yield at temperatures lower than T_t. With *cis*-PA, there was no apolipoprotein specificity in transition suppression, while with *trans*-PA the supression was maximal for apoA-I/DPPC and minimal for apoA-II/DPPC complexes. ApoE-containing complexes were characterized by an intermediate

supression (Table 2). In rHDL particles, the transition shifted to higher temperatures by comparison to pure phospholipid. This shift of 1–2°, detected with *cis*-PA was dependent on F (Fig. 6) or r (Fig. 7) registration and was approximately equal for all three apo/DPPC complexes. With *trans*-PA fluorescence intensity, the shift in the transition temperature was greater for apoA-I/DPPC complexes (5°) than for apoE/DPPC (1.2°) and apoA-II/DPPC (2°) complexes; the analogous shifts were detected by *trans*-PA fluorescence anisotropy (Table 2). Based on hydrophobic matching (Mouritsen and Bloom, 1984), the high 'overmatching' of apoA-I helical segment(s) compared to a mean hydrophobic length of DPPC acyl chains with a preferential interaction of apolipoprotein with phospholipid molecules in a gel state can be suggested while the length of apoA-II segments seems to be more balanced. Protein–lipid interactions for all apolipoproteins studied resulted in a more disordered lipid bilayer at $T < T_t$. The bilayer was more ordered at temperatures above the transition temperature as evidenced by r measurements with both probes (Fig. 7); however, the disordering effect of the protein was much more evident with *trans*-PA.

The individual effect of apolipoprotein on the cooperativity of DPPC phase transition in ternary apoA-I/DPPC/Chol complexes was studied by varying the apoA-I content but keeping Chol content constant. The entropy changes as a function of apoA-I content up to 9.5 mol apolipoprotein/1000 mol DPPC calculated both from *trans*-PA intensity and anisotropy are given in Fig. 8. (Generally, with a decrease of disc dimensions, the entropy change decreased about twofold; however, ΔS values derived from F measurements, decreased continuously, while ΔS

Table 2
Temperature-induced transition in liposomes and in the complexes with different apolipoproteins detected by fluorescence intensity F and anisotropy r of *cis*- and *trans*-parinaric acids (means ± SEM, the number of separate experiments are indicated in the brackets)

Sample	Probe	By intensity		By anisotropy	
		T_t,(°C)	F_s/F_f	T_t,(°C)	r_s/r_f
DPPC liposome	*cis*-PA (5)	41.1 ± 0.3	1.58 ± 0.06	40.2 ± 0.2	2.14 ± 0.04
	trans-PA (2)	41.5 ± 0.2	3.51 ± 0.08	40.8 ± 0.3	1.98 ± 0.01
DPPC/Chol liposome	*cis*-PA (4)	39.8 ± 0.3	1.54 ± 0.07	38.5 ± 0.2	1.86 ± 0.02
	trans-PA (4)	40.3 ± 0.1	2.86 ± 0.12	39.2 ± 0.2	1.62 ± 0.03
A-I/DPPC	*cis*-PA (2)	43.2 ± 0.1	1.42 ± 0.003	42.3 ± 0.3	1.51 ± 0.13
	trans-PA (2)	46.4 ± 1.8	2.66 ± 0.20	44.7 ± 1.7	1.19 ± 0.00
A-I/DPPC/Chol	*cis*-PA (2)	43.2 ± 0.1	1.32 ± 0.14	37.1 ± 4.5	8.51 ± 5.16
	trans-PA (2)	42.2 ± 0.0	2.19 ± 0.06	39.7 ± 0.4	1.13 ± 0.04
E/DPPC	*cis*-PA (1)	42.4	1.34	41.1	1.46
	trans-PA (1)	42.7	3.04	40.8	1.37
E/DPPC/Chol	*cis*-PA (1)	42.0	1.28	41.6	1.80
	trans-PA (1)	42.4	2.07	40.3	1.21
A-II/DPPC	*cis*-PA (3)	43.3 ± 0.1	1.35 ± 0.09	42.7 ± 0.1	1.45 ± 0.07
	trans-PA (2)	43.5 ± 0.2	3.74 ± 0.15	41.6 ± 0.0	1.31 ± 0.04
A-II/DPPC/Chol	*cis*-PA (2)	41.3 ± 1.6	1.36 ± 0.03	44.9 ± 2.1	2.07 ± 0.49
	trans-PA (2)	43.8 ± 0.5	1.54 ± 0.14	42.3 ± 0.5	1.46 ± 0.15

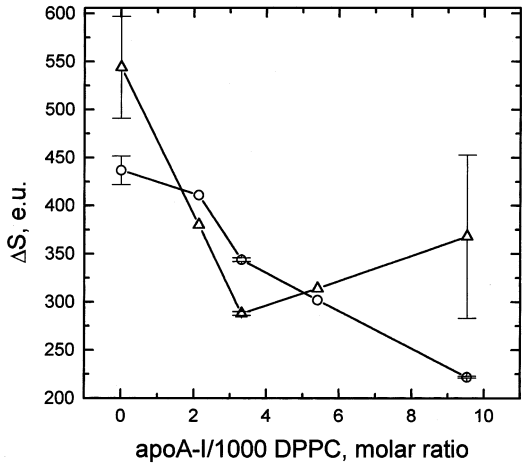

Fig. 8. The concentration dependence of entropy change ΔS in apoA-I/DPPC/Chol complexes with different apolipoprotein content measured by *trans*-PA fluorescence intensity F (circle) and anisotropy r (triangle). Cholesterol content varied between 9 and 12 molecules per 100 DPPC molecules, e.u., entropy unit (cal/K mol).

derived from r measurements reached plateu.) As followed from ΔS changes, the increase of apoA-I fraction in rHDL particles led to a decrease in cooperativity of DPPC phase transition, probably due to the decrease in size of the lipid bilayer and/or to a decrease in the interactions between DPPC molecules in the particle compared to pure bilayer. The latter effect may result in the expansion of the lipid phase in rHDL at $T < T_t$ (Dergunov and Dobretsov, 2000).

In ternary apo/DPPC/Chol complexes, by comparison to apo/DPPC counterparts, the magnitude of the transition influenced both by apolipoprotein and cholesterol and detected by *cis*-PA fluorescence intensity (Fig. 6) decreased most profoundly for apoA-I- but did not change for apoA-II-containing complexes (Table 2). The transition temperatures were also lower, but compared to transition amplitude changes, the direction of the T_t changes was quite opposite. For *trans*-PA, the changes in amplitude and in the transition temperature were opposite to changes in these parameters detected by *cis*-PA, i.e. F_s/F_f decreased most significantly for apoA-II/DPPC/Chol but T_t did not change for this complex (Fig. 6, Table 2).

4. Discussion

4.1. Cholesterol localization and influence on the DPPC dynamics in apoA-I-containing rHDL

The heterogeneous organization of the lipid phase of the Chol-free rHDL assumes the existence of two separate regions differing in lipid dynamics, i.e. a boundary lipid region in close proximity to apolipoprotein and the rest of the bilayer (Dergunov and Dobretsov, 2000). At $T < T_t$ in the present study for apoA-I/DPPC/Chol particles, the data correspond to R value of 5.4 nm and to the accumulation of cholesterol molecules in the central area with a radius of 2.8 nm. Partial (Massey et al., 1985) or complete cholesterol exclusion from the boundary layer (Tall and Lange, 1978) has been suggested. The upper value for Chol content in bulk lipid can be estimated based on the following assumptions: (1) the total area of this domain on two disc surfaces is $2(\pi \times 2.8^2) = 49$ nm^2; (2) the surface area varies between 0.25 and 0.40 nm^2 for each of 18.4 cholesterol molecules which are contained in rHDL particle (Dergunov et al., 1997) and is dependent on a cholesterol-condensing effect (Demel et al., 1982; Lapshin et al., 1983) that contributes to 6 from 49 nm^2. The remaining 43 nm^2 are occupied by phospholipid molecules; (3) the surface area occupied by an individual DPPC molecule is close to 0.65 nm^2 (Lapshin et al., 1983; Dobretsov et al., 1989). Hence, 66 ($= 43/0.65$) DPPC molecules belong to the central disc area enriched in cholesterol. The Chol/DPPC molar ratio for this area is equal to $18.4/66 = 0.28$, i.e. 22 mol.% Chol that exceeds three times the mean value for the whole lipid phase. The boundary lipid and the rest of the bilayer in rHDL particle have been suggested to contain lower than 8 and 22 mol.% cholesterol, respectively. It is interesting to compare the value for bulk lipid domain with the boundary limits of cholesterol content in DPPC/Chol mixed bilayers, namely 7.5–20 mol.% that corresponded to co-existence of phases with heterogeneous Chol distribution within DPPC bilayer (Ipsen et al., 1987; Vist and Davis, 1990). So, it is reasonable to assume that boundary lipid is characterized by

low cholesterol content while Chol-rich and -free phases co-exist in the central part of rHDL particle. The cholesterol enrichment of the central part of the particle still persists after DPPC phase transition as evidenced by both probes. The data on the dimensions of lipid phase and the regions of preferential location of parinaric acid probes, together with the estimates of probe dynamics with or without cholesterol are summarized in Table 3. Protein–lipid interactions due to the presence of apolipoprotein molecule in the complex at $T > T_t$ seems to induce the steric hindrance in DPPC bilayer due to the rigid apolipoprotein surface. At temperatures lower than the phospholipid transition temperature, probe mobility in rHDL increased significantly compared to liposomes probably due to a lower cooperative interaction in the lipid part of the complex. Furthermore, the primary contribution of cooperative phenomena and apolipoprotein to probe mobility in rHDL at temperatures lower and higher T_t, respectively is suggested.

Three experimental findings in this study are principal to describe the relationship between cholesterol and phospholipid in apoA-I-containing rHDL: (i) the accumulation of *trans*-PA in DPPC-rich phase in Chol-containing liposomes at $T < T_t$; (ii) the different location both of *cis*- and *trans*-PA in Chol-free and -containing rHDL; and (iii) the prominent 'overmatching' of apoA-I helical segments. While the phase behaviour of DPPC and Chol molecules was described based on probe distribution, other alternatives cannot be excluded. Moreover, the hydrophobic matching concept may possess only a limited value due to the uncertainty about the exact location of apolipoprotein helical segments relative to phospholipid acyl chains in discoidal rHDL.

We suggest a partial inclusion of cholesterol molecules into boundary lipid consistent with the existence of two separate Chol-free and -containing regions in the latter, based on a larger occupancy region for *trans*-PA by comparison to *cis*-PA in apoA-I/DPPC/Chol complexes. Whether they exist as Chol-binding sites on apoA-I or are organized into separate domains, their relative dimensions cannot be discriminated. Anyway, the apolipoprotein-induced decrease of lipid molecular order for Chol-containing sites in boundary lipid at $T < T_t$ may be counterbalanced by cholesterol molecules with their 'ordering' effect for fluid-like lipid environment. A 4:1 DPPC/Chol stoichiometry may exist for these Chol-containing sites (Hyslop et al., 1990). So, at low temperatures cholesterol increases the molecular order in disordered boundary lipid region at the disk periphery, while it induces a disordering effect at the particle centre. Two *trans*-PA-accessible areas, namely, Chol-containing boundary lipid in the periphery and the more centered DPPC-rich phase while only one, Chol-free site in boundary lipid, for *cis*-PA seem to exist. After DPPC phase transition, *trans*-PA moves away from protein surface to more ordered Chol-rich

Table 3
Preferential localization and degree of wobbling-type motion of parinaric acid probes in apoA-I-containing rHDL

Temperature (°C)	Cholesterol (mol.%)	Radius of the lipid phase (nm)	Probe localization (nm)		γ (°)		Reference
			trans-PA	*cis*-PA	*trans*-PA	*Cis*-PA	
25	0	5.0	0–4.0	1.7–5.0	28	28	Dobretsov et al., 1998
	8	5.4	2–5.4	3.7–5.4	28	28	This paper
50	0	5.2	0–5.2	0–5.2	37	42	Dergunov and Dobretsov, 2000
	8	5.4	0–5.0	1.5–5.4	37	43	This paper

The probe localization as a distance from particle axis was measured by energy transfer and probe partition. The amplitude of wobbling-type motion of the probe molecule inside the conical volume is characterized by the γ angle.

phase while *cis*-PA remains in the boundary lipid. The presumed probe distribution assumes an incomplete phase separation between Chol-free and -containing regions in boundary lipid or, in terms of binding sites, their heterogeneous radial distribution. Hence, these results suggest a heterogeneous cholesterol distribution both in boundary and bulk lipid of apoA-I-containing rHDL.

Two alternatives can be proposed as a driving force for cholesterol partial inclusion into boundary lipid region in apoA-I-containing discoidal particles, i.e. a metastable state of the lipid phase or a comparable degree of interaction between DPPC or Chol molecules with apoA-I. The second alternative seems to be more realistic with the following experimental support: (1) the DMPC–Chol mixture possessed maximum affinity to apoA-I (Pownall et al., 1979); (2) the fluorescent Chol analogue preferentially accumulated in the central part of apoA-I/DMPC discs (Massey et al., 1985), the ratio of the relative affinities of Chol and DMPC to apoA-I was equal to 0.67, which lies within the range suggested by our study; (3) the cholesterol influence on the association of apoA-I with DPPC (Van Tornout et al., 1980) or egg yolk PC (Saito et al., 1997), on the apoprotein lysine microenvironment (Sparks et al., 1993) and on the antibody binding (Bergeron et al., 1995) was mentioned; (4) the ratio of PC- to Chol-binding sites on pig apoA-I was equal to 40:1 (Handa et al., 1992).

4.2. Lipid phase state in complexes with different apolipoproteins

The specific structure of each apolipoprotein resulted both in a different degree of immobilization of the nearest phospholipid molecules around the hydrophobic face of apolipoprotein molecule with a different cholesterol distribution in the plane of the bilayer and in a production of the complexes of different size. In the latter case, cholesterol inclusion under the quantities applied had only a minor effect on the complex dimensions (Dergunov et al., 1997; Sparks et al., 1993). For apoA-I/DPPC/Chol, apoE/DPPC/Chol and apoA-II/DPPC/Chol complexes, the complex with apoA-II had the highest supression of temperature-induced response of fluorescence intensity of *trans*-PA and a minimal supression of *cis*-PA response (Fig. 6, Table 2). In apoA-I-containing complex, *cis*-PA localizes mainly in boundary lipid and *trans*-PA distributes between boundary lipid and bulk bilayer. In apoA-II/DPPC/Chol complex *cis*-PA distributes between two lipid regions and *trans*-PA localizes preferentially in the boundary lipid. For apoE-containing rHDL, the probe distribution was described by an intermediate situation. This different mode of probe distribution may possibly be related to differential exclusion of cholesterol from boundary lipid in the complexes with different apolipoproteins. In this case, the interaction of apoA-II with phospholipid may be tighter compared to the interaction of apoA-I with phospholipid. Cholesterol does not influence the former interaction as has been observed experimentally (Van Tornout et al., 1980). Overall, the magnitude of overmatching differs for the apolipoproteins studied and appears to be minimal for apoA-II and maximal for apoA-I, ranged by T_t value. Cholesterol and apoA-I (but not apoA-II) molecules efficiently compensate each other for the opposite changes in matching to DPPC acyl chain length that could explain the relative enrichment of boundary layer with Chol in the discs with apoA-I compared to apoA-II/DPPC/Chol particles.

The different mode of interaction of apoA-I and apoA-II with DPPC and the different cholesterol content in these complexes could result in different substrate properties of rHDL in the LCAT reaction. A 20-fold decrease of enzyme activity in the apoA-II-complexes by comparison to the apoA-I-complexes has been observed (Jonas et al., 1984). The existence of multiple sites in apoA-I molecule with different affinities to cholesterol and phospholipid has been suggested recently (Meng et al., 1995). We suggest the same situation in the case of apoE. The differences in the functional properties of the complexes with apoA-I and apoE (De Pauw et al., 1997) could originate from the different intradomain organization of these apolipoprotein molecules. As a result, the local concentration of cholesterol molecules and/or their orientation and mobility in close vicinity to cholesterol-binding sites could differ in these two complexes.

5. Conclusion

The data obtained indicate that: (1) the inclusion of 8 mol.% of cholesterol did not significantly change both the particle dimensions (13 ± 1 nm) and the mean distance between apoA-I and disc axis; (2) despite the limited number of DPPC molecules in rHDL, the lipid part of this particle seems to possess the usual properties of lipid continuum found in biological membranes. The presence of boundary lipid in close proximity to apoA-I molecule with the partial exclusion of cholesterol molecules from this region is a prominent feature of the discoidal rHDL particle. The heterogeneous cholesterol distribution both in boundary and bulk lipid is presumed; (3) *cis*- and *trans*-PA distribute differently into various lipid domains in rHDL with high sensitivity of *trans*-PA to immobilized regions; (4) the intimate temperature-dependent balance between the matching of the effective hydrophobic length of DPPC and cholesterol molecules and apolipoprotein helical regions is believed to be responsible for the action of Chol and apolipoprotein molecules on the dynamic and phase properties of DPPC bilayer; (5) the different Chol distributions between boundary and bulk lipid, suggested for rHDL with different apolipoproteins, do not seem to depend on complex dimensions but rather on the apolipoprotein structure. The mode of Chol distribution in these complexes needs additional, more direct experimental confirmation. Since these results are based mainly on the parinaric probe behaviour, experiments to localize fluorescent Chol analogues in rHDL with different apolipoproteins are now in progress.

Acknowledgements

We are grateful to Dr M. Rosseneu (Laboratorium voor Lipoproteine Chemie/Vakgroep Biochemie, Universiteit Gent, Belgium) for allowing us to use the facilities in her laboratory. Thanks are also due to Dr B. Vanloo who participated in the initial phase of the experiments. The excellent technical assistance of J. Taveirne and H. Caster is acknowledged. We thank also S. Kolis and G. Ehrlich for their kind help in language correction. This work was supported partially by Russian Fund for Basic Research, grant 01-04-48140.

References

Bergeron, J., Frank, P.G., Scales, D., Meng, Q.-H., Castro, G., Marcel, Y.L., 1995. Apolipoprotein A-I conformation in reconstituted discoidal lipoproteins varying in phospholipid and cholesterol content. J. Biol. Chem. 270, 27 429–27 438.

Borhani, D.W., Rogers, D.P., Engler, J.A., Brouillette, C.G., 1997. Crystal structure of truncated human apolipoprotein A-I suggests a lipid-bound conformation. Proc. Natl. Acad. Sci. USA 94, 12 291–12 296.

Brasseur, R., De Meutter, J., Vanloo, B., Goormaghtigh, E., Ruysschaert, J.M., Rosseneu, M., 1990. Mode of assembly of amphipathic helical segments in model high-density lipoproteins. Biochim. Biophys. Acta 1043, 245–252.

Brasseur, R., Lins, L., Vanloo, B., Ruysschaert, J.M., Rosseneu, M., 1992. Molecular modeling of the amphipathic helices of the plasma apolipoproteins. Proteins: Struct. Funct. Genet. 13, 246–257.

Davidson, W.S., Arnvig-McGuire, K., Kennedy, A., Kosman, J., Hazlett, T.L., Jonas, A., 1999. Structural organization of the N-terminal domain of apolipoprotein A-I: studies of tryptophan mutants. Biochemistry 38, 14 387–14 395.

Davidson, W.S., Hazlett, Th., Mantulin, W.W., Jonas, A., 1996. The role of apoprotein AI domains in lipid binding. Prot. Natl. Acad. Sci. USA 93, 13 605–13 610.

De Pauw, M., Vanloo, B., Dergunov, A.D., Devreese, A.-M., Baert, J., Brasseur, R., Rosseneu, M., 1997. Composition and structural and functional properties of discoidal and spherical phospholipid-apoE3 complexes. Biochemistry (Moscow) 62, 251–263.

Demel, R.A., Bruckdorfer, K.R., vanDeenen, L.L., 1982. Structural requirements of sterol for the interaction with lecithin at the air–water interface. Biochim. Biophys. Acta 255, 311–320.

Dergunov, A.D., Aniskovich, L.P., Shuvaev, V.V., 1990. Affinity chromatography on heparin–sepharose under reducing conditions as a method of selective enrichment with individual isoforms of apolipoprotein E. Bull. Exp. Biol. Med. 110, 894–898.

Dergunov, A.D., Dobretsov, G.E., 2000. Apolipoprotein A-I localization and dipalmitoylphosphatidylcholine dynamics in reconstituted high density lipoproteins. Chem. Phys. Lipids 104, 161–173.

Dergunov, A.D., Taveirne, J., Vanloo, B., Caster, H., Rosseneu, M., 1997. Structural organization of lipid phase and protein–lipid interface in apolipoprotein–phospholipid recombinants: influence of cholesterol. Biochim. Biophys. Acta 1346, 131–146.

Dobretsov, G.E., Dergunov, A.D., Taveirne, J., Caster, H., Vanloo, B., Rosseneu, M., 1998. Apolipoprotein localiza-

tion in reconstituted HDL particles: fluorescence energy transfer study. Chem. Phys. Lipids 97, 65–77.

Dobretsov, G.E., Kurek, N.K., Machov, V.N., Syrejshchikova, T.I., Yakimenko, M.N., 1989. Determination of fluorescent probes localization in membranes by nonradiative energy transfer. J. Biochem. Biophys. Meth. 19, 259–274.

Dumas, F., Lebrun, M.C., Tocanne, J.-F., 1999. Is the protein/lipid hydrophobic matching principle relevant to membrane organization and functions? FEBS Lett. 458, 271–277.

Fielding, C.J., Fielding, P.E., 1995. Molecular physiology of reverse cholesterol transport. J. Lipid Res. 36, 211–228.

Gil, T., Ipsen, J.H., Mouritsen, O.G., Sabra, M.C., Sperotto, M.M., Zuckermann, M.J., 1998. Theoretical analysis of protein organization in lipid membranes. Biochim. Biophys. Acta 1376, 245–266.

Gliss, C., Randel, O., Casalta, H., Sackmann, E., Zorn, R., Bayerl, T., 1999. Anisotropic motion of cholesterol in oriented DPPC bilayers studied by quasielastic neutron scattering: the liquid-ordered phase. Biophys. J. 77, 331–340.

Handa, T., Saito, H., Tanaka, I., Kakee, A., Tanaka, K., Miyajima, K., 1992. Lateral interactions of pig apolipoprotein A-1 with egg yolk phosphatidylcholine and with cholesterol in mixed monolayers at the triolein–saline interface. Biochemistry 31, 1415–1420.

Hyslop, P.A., Morel, B., Sauerheber, R.D., 1990. Organization and interaction of cholesterol and phosphatidylcholine in model bilayer membranes. Biochemistry 29, 1025–1038.

Ipsen, J.H., Karlström, G., Mouritsen, O.G., Wennerström, H., Zuckermann, M.J., 1987. Phase equilibria in the phosphatidylcholine–cholesterol system. Biochim. Biophys. Acta 905, 162–172.

Johnson, W.J., Mahlberg, F.H., Rothblat, G.H., Phillips, M.C., 1991. Cholesterol transport between cells and high-density lipoproteins. Biochim. Biophys. Acta 1085, 273–298.

Jonas, A., 1992. Lipid-binding properties of apolipoproteins. In: Rosseneu, M. (Ed.), Structure and Function of Apolipoproteins. CRC Press, Boca Raton, Ann Arbor, London, Tokyo, pp. 217–250.

Jonas, A., Sweeny, S.A., Herbert, P.N., 1984. Discoidal complexes of A and C apolipoproteins with lipids and their reactions with lecithin:cholesterol acyltransferase. J. Biol. Chem. 259, 6369–6375.

Keough, K.M., Davis, P.J., 1979. Gel to liquid-crystalline phase transitions in water dispersions of saturated mixed-acid phosphatidylcholines. Biochemistry 18, 1453–1459.

Killian, J.A., 1998. Hydrophobic mismatch between proteins and lipids in membranes. Biochim. Biophys. Acta 1376, 401–415.

Kinosita, K., Kawato, S., Ikegami, A., 1977. A theory of fluorescence polarization decay in membranes. Biophys. J. 20, 289–305.

Laemmli, U.K., 1970. Cleavage of structural proteins during the assembly of the head of bacteriophage T4. Nature 227, 680–685.

Lakowicz, J.R., 1983. Principles of Fluorescence Spectroscopy. Plenum Press, New York.

Lapshin, E.N., Dobretsov, G.E., Klebanov, G.I., Vladimirov, Yu.A., 1983. 'Decondensing' effect of cholesterol on bilayer of the total egg phospholipids. Biophysics (Moscow) 28, 752–755.

Mantulin, W.W., Pownall, H.J., Jameson, D.M., 1986. Fluorescence quenching studies of apolipoprotein A-I in solution and in lipid–protein complexes: protein dynamics. Biochemistry 25, 8034–8042.

Massey, J.B., She, H.S., Gotto, A.M. Jr., Pownall, H.J., 1985. Lateral distribution of phospholipid and cholesterol in apolipoprotein A-I recombinants. Biochemistry 24, 7110–7116.

Matz, C.E., Jonas, A., 1982. Micellar complexes of human apolipoprotein A-I with phosphatidylcholines and cholesterol prepared from cholate–lipid dispersions. J. Biol. Chem. 257, 4535–4540.

McMullen, T.P.W., Lewis, R.N.A.H., McElhaney, R.N., 1993. Differential scanning calorimetric study of the effect of cholesterol on the thermotropic phase behavior of a homologous series of linear saturated phosphatidylcholines. Biochemistry 32, 516–522.

McMullen, T.P., McElhaney, R.N., 1995. New aspects of the interaction of cholesterol with dipalmitoylphosphatidylcholine bilayers as revealed by high-sensitivity differential scanning calorimetry. Biochim. Biophys. Acta 1234, 90–98.

Meng, Q.-H., Bergeron, J., Sparks, D.L., Marcel, Y.L., 1995. Role of apolipoprotein A-I in cholesterol transfer between lipoproteins. Evidence for involvement of specific apoA-I domains. J. Biol. Chem. 270, 8588–8596.

Mouritsen, O.G., Bloom, M., 1984. Mattress model of lipid–protein interactions in membranes. Biophys. J. 46, 141–153.

Pownall, H.J., Massey, J.B., Kusserow, S.K., Gotto, A.M., 1979. Kinetics of lipid–protein interactions: effect of cholesterol on the association of human plasma high density apolipoprotein A-I with L-α-dimyristoylphosphatidylcholine. Biochemistry 18, 574–579.

Presti, F.T., Pace, R.J., Chan, S.I., 1982a. Cholesterol–phospholipid interaction in membranes. 1. Cholestane spin-label studies of phase behavior of cholesterol–phospholipid liposomes. Biochemistry 21, 3821–3830.

Presti, F.T., Pace, R.J., Chan, S.I., 1982b. Cholesterol–phospholipid interaction in membranes. 2. Stoichiometry and molecular packing of cholesterol-rich domains. Biochemistry 21, 3831–3835.

Radhakrishnan, A., McConnell, H.M., 1999. Condensed complexes of cholesterol and phospholipids. Biophys. J. 77, 1507–1517.

Radhakrishnan, A., Anderson, T.G., McConnell, H.M., 2000. Condensed complexes, rafts, and the chemical activity of cholesterol in membranes. Proc. Natl. Acad. Sci. USA 97, 12 422–12 427.

Rodriguez, S., Garda, H.A., Heinzen, H., Moyna, P., 1997. Effect of plant monofunctional triterpenes on the dynamic

and structural properties of dipalmitoylphosphatidylcholine bilayers. Chem. Phys. Lipids 89, 119–130.

Rye, K.-A., Jauhiainen, M., Barter, P.J., Ehnholm, C., 1998. Triglyceride-enrichment of high density lipoproteins enhances their remodelling by phospholipid transfer protein. J. Lipid Res. 39, 613–622.

Saito, H., Miyako, Y., Handa, T., Miyajima, K., 1997. Effect of cholesterol on apolipoprotein A-I binding to lipid bilayers and emulsions. J. Lipid Res. 38, 287–294.

Sankaram, M.B., Thompson, T.E., 1990. Interaction of cholesterol with various glycerophospholipids and sphingomyelin. Biochemistry 29, 10 670–10 675.

Schubert, R., Beyer, K., Wolburg, H., Schmidt, K.H., 1986. Structural changes in membranes of large unilamellar vesicles after binding of sodium cholate. Biochemistry 25, 5263–5269.

Segrest, J.P., 1977. Amphipathic helixes and plasma lipoproteins: thermodynamic and geometric considerations. Chem. Phys. Lipids 18, 7–22.

Segrest, J.P., Jones, M.K., Klon, A.E., Sheldahl, C.J., Hellinger, M., De Loof, H., Harvey, S.C., 1999. A detailed molecular belt model for apolipoprotein A-I in discoidal high density lipoprotein. J. Biol. Chem. 274, 31 755–31 758.

Sklar, L.A., Hudson, B.S., Simoni, R.D., 1977. Conjugated polyene fatty acids as fluorescent probes: synthetic phospholipid membrane studies. Biochemistry 16, 819–828.

Sklar, L.A., Miljanich, G.P., Dratz, E.A., 1979. Phospholipid phase separation and the partition of *cis*-parinaric acid and *trans*-parinaric acid among aqueous, solid lipid, and fluid lipid phases. Biochemistry 18, 1707–1716.

Sparks, D.L., Davidson, W.S., Lund-Katz, S., Phillips, M.C., 1993. Effect of cholesterol on the charge and structure of apolipoprotein A-I in recombinant high density lipoprotein particles. J. Biol. Chem. 268, 23 250–23 257.

Sparks, D.L., Davidson, W.S., Lund-Katz, S., Phillips, M.C., 1995. Effects of the neutral lipid content of high density lipoprotein on apolipoprotein A-I structure and particle stability. J. Biol. Chem. 270, 26 910–26 917.

Sparks, D.L., Lund-Katz, S., Phillips, M.C., 1992a. The charge and structural stability of apolipoprotein A-I in discoidal and spherical recombinant high density lipoprotein particles. J. Biol. Chem. 267, 25 839–25 847.

Sparks, D.L., Phillips, M.C., Lund-Katz, S., 1992b. The conformation of apolipoprotein A-I in discoidal and spherical recombinant high density lipoprotein particles. J. Biol. Chem. 267, 25 830–25 838.

Tall, A.R., Lange, Y., 1978. Interaction of cholesterol, phospholipid and apoprotein in high density lipoprotein recombinants. Biochim. Biophys. Acta 513, 185–197.

Van Erpecum, K.J., Carey, M.C., 1997. Influence of bile salts on molecular interactions between sphingomyelin and cholesterol: relevance to bile formation and stability. Biochim. Biophys. Acta 1345, 269–282.

Van Tornout, P., Vercaemst, R., Lievens, M.J., Caster, H., Rosseneu, M., Assmann, G., 1980. Reassembly of human apoproteins A-I and A-II with unilamellar phosphatidylcholine–cholesterol liposomes. Association kinetics and characterization of the complexes. Biochim. Biophys. Acta 601, 509–523.

Virtanen, J.A., Ruonala, M., Vauhkonen, M., Somerharju, P., 1995. Lateral organization of liquid-crystalline cholesterol–dimyristoylphosphatidylcholine bilayers. Evidence for domains with hexagonal and centered rectangular cholesterol superlattices. Biochemistry 34, 11 568–11 581.

Vist, M.R., Davis, J.H., 1990. Phase equilibria of cholesterol/dipalmitoylphosphatidylcholine mixtures: ^{2}H nuclear magnetic resonance and differential scanning calorimetry. Biochemistry 29, 451–464.

Wang, M.M., Sugar, I.P., Chong, P.L., 1998. Role of the sterol superlattice in the partitioning of the antifungal drug nystatin into lipid membranes. Biochemistry 37, 11 797–11 805.

Yeagle, P.L., 1981. Cholesterol rotation in phospholipid vesicles as observed by 13C NMR. Biochim. Biophys. Acta 640, 263–273.